Improvements to Urban Area Characterization Using Multitemporal and Multiangle SAR Images

Fabio Dell'Acqua, *Member, IEEE*, Paolo Gamba, *Senior Member, IEEE*, and Gianni Lisini

***Abstract*—In this paper, we present some improvements to urban area characterization by means of synthetic aperture radar (SAR) images using multitemporal and multiangle datasets. The first aim of this research is to show that a temporal sequence of satellite SAR data may improve the classification accuracy and the discriminability of land cover classes in an urban area. Similarly, a second point worth discussing is to what extent multiangle SAR data allows extracting complementary urban features, exploiting different acquisition geometries. To these aims, in this paper, we show results on the same urban test site (Pavia, northern Italy), referring to a sequence of European Remote Sensing Satellite 1/2 (ERS-1/2) C-band images and to a set of simulated X-band data with a finer spatial resolution and different viewing angles. In particular, the multitemporal data is analyzed by means of a novel procedure based on a neuro-fuzzy classifier whose input is a subset of the ERS sequence chosen using the histogram distance index. Instead, the multiangle dataset is used to provide a better characterization of the road network in the area, overcoming effects due to the orientation of the SAR sensor.**

***Index Terms*—Road extraction, synthetic aperture radar (SAR) image analysis, urban remote sensing.**

I. Introduction

THE NEED FOR remote sensing tools able to explore urban environments and retrieve spatial, temporal, and environmental characteristics is pressing, given the amount of problems, pollution and various phenomena related to these areas. Many of the papers referring to urban area monitoring in technical literature are based on synthetic aperture radar (SAR) data, since the radar all-weather capability is very useful in many disaster management situations. This is particularly true, for instance, while monitoring flooding events [1] and areas where the cloud cover is usually intense. In urban areas, however, the problems of radar imaging (i.e., multiple bouncing, layover, shadowing) are more evident, and make the task more complex; but now multiple SAR datasets are increasingly becoming available, and the use of such datasets may help in improving our capability to characterize the urban environment. Moreover, airborne high-resolution SAR sensors have been tested, and hopefully satellite platforms will soon deliver very similar images in a multitemporal/multipolarization/multiangle format.

In the past few months the European Space Agency has launched and has been testing the ENVISAT satellite, carrying the Advanced SAR (ASAR) sensor, with improved capabilities with respect to the existing European Remote Sensing Satellite 2 (ERS-2). Moreover, the Italian and the French Space Agencies are funding the realization of the COSMO/SkyMed satellite constellation [2], constituted by satellites partly equipped with visible and multispectral sensors, and partly with an X-band, multipolarization SAR. Finally, the German Aerospace Agency (DLR) and Astrium are starting their work on TerraSAR, a satellite that will fly in polar orbit and provide high-quality X-band images, completing a world coverage every third day [3].

According to these projects and plans, there will be a large amount of SAR datasets recorded at different dates and with different viewing angles. So, this paper aims at investigating the usefulness of multiple SAR datasets for urban characterization by analyzing data collected or simulated over the same urban test site. Setion II is devoted to presenting these images, while the Section III presents the experimental results on multitemporal and multiangle sets, separately. Finally, Section IV concludes the paper discussing the achievements of this research as well as future working directions.

II. Multitemporal/Multiangle SAR Data Over an Urban Test Site

All the SAR images considered in this research were collected or simulated over the urban area of Pavia (northern Italy). The site has been chosen because it well represents the diversity of urban land covers, uses, and features. Pavia is a small town with a very densely built center, some residential areas, industrial suburbs, and the Ticino River runs across it. On this site a large collection of remote sensing data, ranging from airborne to satellite images at different spatial resolution, has been collected in the last years [4]. In particular, extensive ground truthing was carried out, starting from the regional technical map provided by the geographic service of the Lombardia region. The map was used to manually classify the area of interest. The evaluation indexes are, thus, computed on a ground truth large enough to be statistically significant.

A human interpreter is able to produce from the regional map a ground truth for land use, but we cannot extract this information from our test set. As a matter of fact, the available literature and our experience also show that it is not possible in the original ERS data to discriminate with a classification tool between residential and commercial areas, as well as between roads and railways. Moreover, road extraction is strongly dependent on the spatial resolution and the relative orientation between road axes and the satellite sensors. Finally, in this paper the goal is not to provide a new, more accurate classification tool, but to investigate the usefulness of multiple image sets, assessing the advan-

Manuscript received September 17, 2002; revised December 13, 2002. This work was supported the Italian Space Agency (ASI) under contracts ECOSAR and ASI I/R/063/01.

The authors are with Dipartimento di Elettronica, Università di Pavia, 1-27100 Pavia, Italy.

Digital Object Identifier 10.1109/TGRS.2003.814631

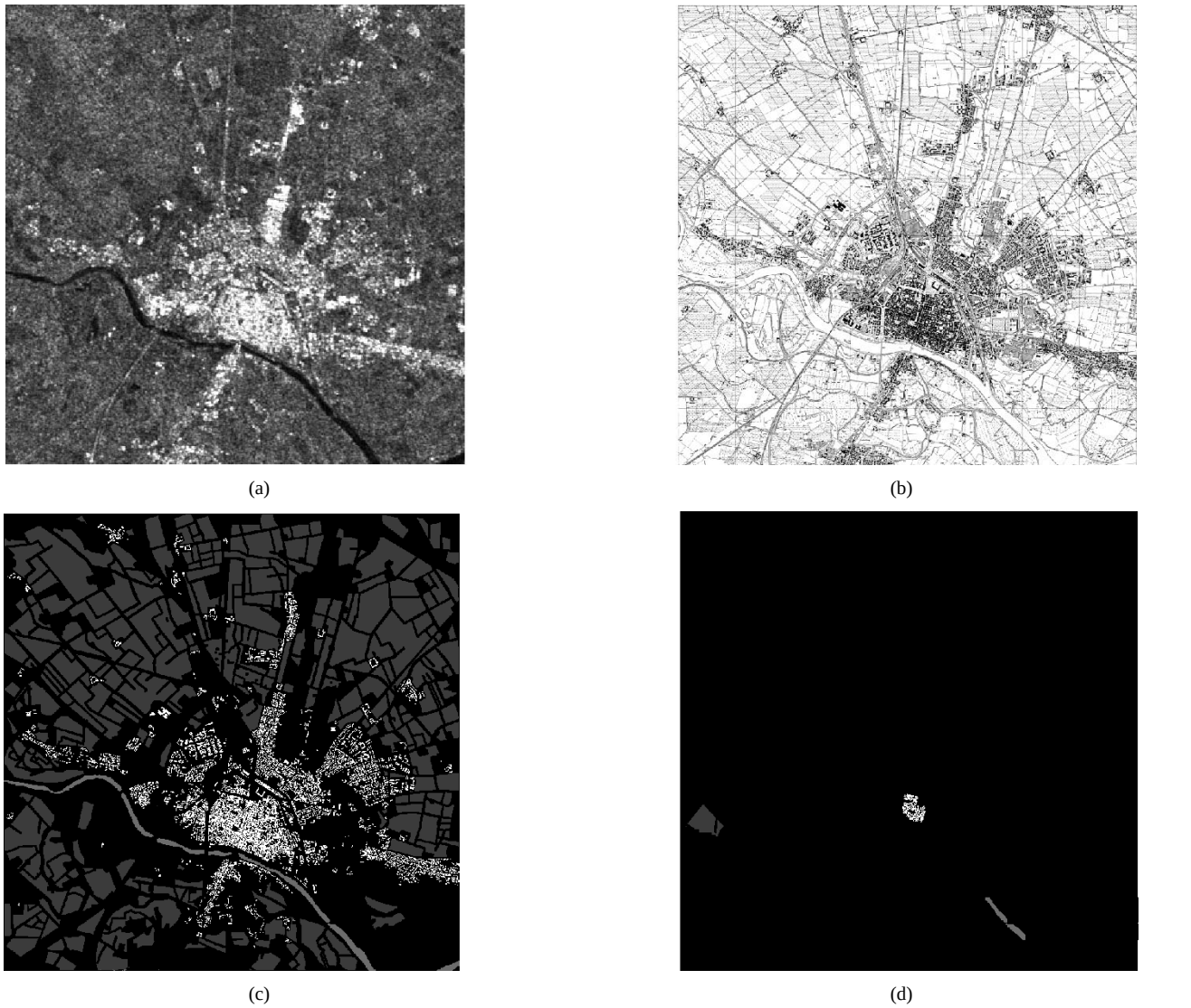

Fig. 1. Data and ground truth available on the test site for this investigation, the town of Pavia (northern Italy). (a) A sample ERS-1 image. (b) The regional technical map on the same area. (c) The detailed ground truth extracted from the latter (classes and colors described in the text). (d) The training set.

tages of having more data on a given area. We, thus, used a simplified land cover ground truth, with only very basic land cover classes. Open water is colored in light gray, and corresponds to the Ticino River, flowing south of the town, and the canal connecting Milan to the river, on the right of the image. Dark gray represents all the different agricultural land usages. Finally, we considered in white the built up areas all over the image.

On this urban test site a multitemporal set of seven ERS-1/2 SAR images have been acquired, covering a time period between 1992 and 2000. The images, recorded either in raw or in single look complex format were all converted to multilook ground range images. For our purposes, we considered a portion of each image covering the town and its surroundings (nearly 800×800 pixels, i.e., more than 65 km^2). These portions were extracted after registering the original data to a version of the ground truth with the same spatial resolution (12.5 m in both main directions). Note that the dataset was originally collected for SAR application to flood characterization, and the dates of the acquisitions correspond to pre- and post-event images for each of the flooding events in years 1992, 1993, and 1994 and only to post-event data for the year 2000. An example of the SAR data, the regional map, the ground truth and the training set are shown in Fig. 1.

The second dataset corresponds to simulated data computed using a SAR simulator [5] capable of providing images similar to the ones that will be delivered by the X-band COSMO/SkyMed sensor. This simulator can take into account the multiple bounce effects typical of an urban environment. The inputs to the simulation were a LIDAR digital terrain model (DTM) of the town and a CAD model of the city center. The output is a set of single look SAR images depicting the same part of the town with different viewing angles at a ground resolution of nearly 3 m. In the following we consider only three views of the same portion of the town, labeled 0°, 40°, and 90° according to the angle between the flight path and the geographical North. This set allows us discussing very basic effects of viewing angles on urban feature extraction. The 0° image is shown in Fig. 2(a). Note that it represents only the city center (nearly 10 km^2). Fig. 2(b) shows a portion of Fig. 1(a), zoomed at the same resolution.

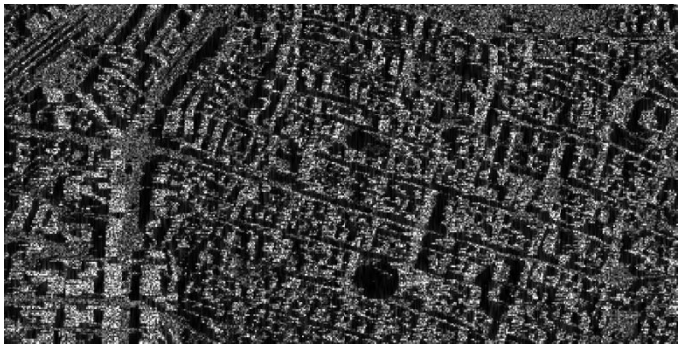

(a)

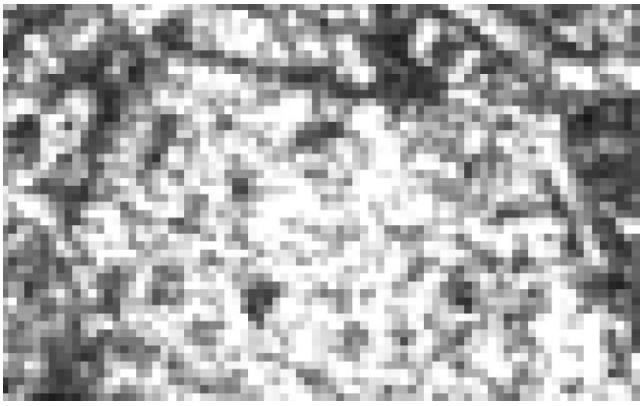

(b)

Fig. 2. (a) Simulated COSMO/SkyMed X-band VV image (2.8-m ground resolution). (b) Zoom on the same town portion from Fig. 1(a) (originally at 12.5-m ground resolution).

III. Urban Analysis by Multiple SAR Images: Methodologies and Experimental Results

As noted in the introduction, multiple images of the same area will soon be delivered by current and future SAR sensors. This will allow exploiting data redundancy and possibly reduce errors in urban area characterization. Multitemporal and multiangle datasets can improve urban analysis in very different ways. As a matter of fact, a sequence of satellite SAR images taken at different dates from almost the same flight path is invaluable for change detection, area monitoring and target recognition. On the other hand, SAR artifacts due to the viewing geometry hold unaffected and we cannot recover from their effects. Multiangle images allow instead getting around these problems by displaying different details of the same scene. For instance, the street network at different viewing angles on the same area has very different appearance, and we may use these views to gain a better knowledge of the whole road map. Therefore, in the following we will present two applications, namely multitemporal ERS data classification and multiview road map extraction. In each subsection, we will present first the methodology used for the application, and then some experimental results. This choice follows from the application-oriented nature of this research work.

A. Urban Land Cover Classification by Means of Multitemporal SAR Data

In technical literature many examples are reported dealing with change analysis in multitemporal SAR data, while only a few papers are devoted to exploiting the stability of some features in radar images that may be useful to improve with successive data acquisitions the classification as well as the characterization accuracy. This has been used for forest [6] as well as agricultural [7] applications. Moreover, the decorrelation between acquisitions of the same stable feature, and due to the geometry of acquisition and the terrain have been investigated in [8]. In an urban area, however, there have been only studies on the decorrelation of anthropogenic features, mainly based on interferometric dataset in [9] and [10]. So, the main approach in these areas is the Permanent Scatterers technique [11], useful for fine-precision, three-dimensional analysis of ground subsidence and terrain movements. In this technique, however, a minor fraction of the original data is used to improve the understanding of the whole images, but it is possible to extract two-dimensional features (say, roads and blocks) only indirectly. In this paper, we propose a novel technique to deal directly with multitemporal data to improve the classification accuracy of urban areas.

The overall structure of this algorithm is outlined in Fig. 3. It is composed of a first evaluation step followed by a successive classification procedure. The idea is that, if the image sequence is long enough, and we have some knowledge of the structures we would like to extract, using all the data in the sequence could mean overkilling the problem, and maybe some part of the sequence could be ignored. To make such a choice, however, we need to define a strategy, that we based on the computation of the histogram distance index (HDI), in a simplified version with respect to the one proposed in [12]

$$\mathrm{HDI} = \left(1 - \sum_{x} \min(f(x), g(x))\right) \cdot 100. \tag{1}$$

In (1), $f(x)$ and $g(x)$ are the probability density functions of the gray levels of the pixels contained in the training sets of the two images to be compared. The value of HDI ranges between 0 and 100 as a function of the superposition of the histograms. If $f(x)$ and $g(x)$ are the same function, the resulting HDI value will be zero, while if their supports do not intersect, the value will be 100.

We compute HDI values considering training areas for each ground truth class in single-date and multidate image sets. Therefore, $f(x)$ may be in our case the probability density function for vegetation training areas, where $x = \{x_1, x_2, \ldots, x_L\}$ is the vector of gray values for a combination of L multitemporal images. By comparing the mean of the HDI values for any pair of training classes, and reordering it for any possible combination of the multitemporal ERS data constituting our dataset, we want to know if we can obtain a criterion to choose the best data combination for our urban classification purposes.

To get a first assessment of the usefulness of HDI for input selection, following the work flow in Fig. 3 we computed this index for all the combinations of seven images. For sake of simplicity, we report in Table I the HDI values only for all the possible image pairs. The HDI value should be correlated with the overall accuracy obtained by means of a neural supervised classifier [13], [14]. Moreover, in the same table we list for comparison the Jeffrey–Matsushita distance for the same training set. Even if it is not very evident, there is a correlation

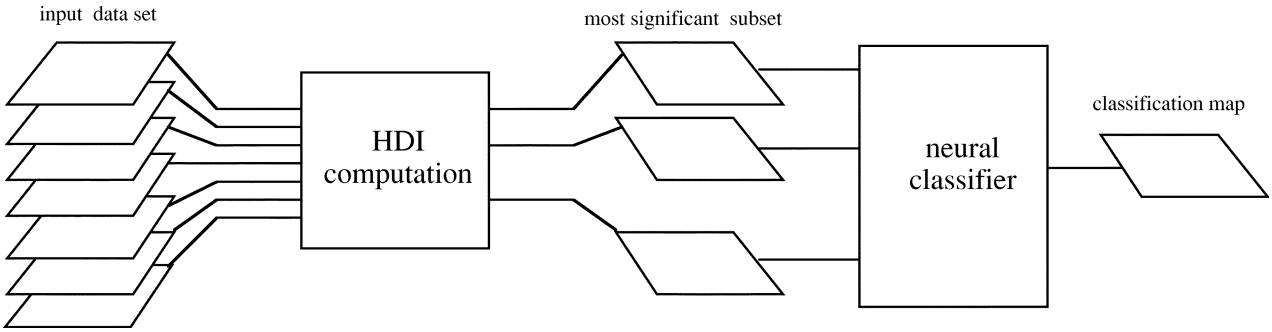

Fig. 3. Work flow of the procedure proposed in this paper to analyze a multitemporal set of images.

TABLE I
HDI AND JEFFREY–MATSUSHITA (J–M) DISTANCE VALUES FOR ANY COMBINATION OF TWO OUT OF SEVEN SAR IMAGES. IMAGES ARE NAMED BY THEIR RECORDING DATE, AND COMBINATIONS ARE ORDERED ACCORDING TO OVERALL CLASSIFICATION ACCURACY

Combination	Overall accuracy	HDI	J-M
931111+001028	67.560	95.71	1.6980
921022+931111	71.490	95.40	1.6550
930624+001028	73.290	96.65	1.7187
930624+931111	73.500	97.82	1.7497
941109+930624	74.710	98.07	1.7639
941109+941003	74.970	96.79	1.6672
941003+001028	75.980	95.15	1.6448
921022+930624	76.410	97.32	1.7334
941003+921022	76.800	96.10	1.6412
921022+001028	77.060	95.12	1.6696
941109+931111	77.720	96.93	1.7079
941003+931111	77.800	95.68	1.6545
941109+001028	79.030	96.32	1.7293
920813+931111	79.110	98.21	1.7728
941109+921022	79.260	96.51	1.7001
941003+930624	79.650	98.10	1.7461
941109+920813	85.390	98.38	1.7662
920813+001028	85.400	98.21	1.7793
921022+920813	86.800	98.21	1.7651
920813+930624	87.770	98.66	1.7841
941003+920813	88.910	98.38	1.7420

$(\rho_{\mathrm{HDI}} = 0.66)$ between the sequence of HDI values and the overall accuracy. Moreover, this correlation is higher between the Jeffrey–Matsushita distance values and the same accuracy $(\rho_{\mathrm{JM}} = 0.56)$. An even lower correlation is obtained for transformed divergence (not shown in the table). These values suggest the idea that HDI can be used as a sufficiently reliable tool to guess which is the subset of the image sequence most useful for our classification purposes. The tool actually is not perfect: the correlation coefficient is quite low and the ordered sequence of image pairs with respect to HDI is different from the one obtained using the overall accuracy. However, it has advantage over some other indexes.

The classification map for the best image pair, after optimizing the neural classifier parameters [13], [14] is shown in Fig. 4(b), while Table II contains the corresponding confusion matrix. We can compare this result with the best single-date confusion matrix (Table III) and classification map [Fig. 4(a)] (presented in [15]). Of course, the use of more than one ERS image on the urban test site provides a better characterization of any of the three considered classes. In particular, there is a net advantage in the detection of the built areas (omission accuracy increases by more than 5%), and a similar refinement for the river $(+5.3\%)$. It should be noted, however, that not only the choice of the subset is important, but also the method to exploit the information hidden in the chosen subset. For instance, the results for a multiband classification of three images is different than the one-dimensional classification of the data obtained by applying a temporal median filter to the same set. The overall accuracy values are 91.71%, and 77.57%, respectively. It is clear that the pattern recognition capability of our neural classifier works better on multiband data.

To add a computational note, it is worth stressing that using a multitemporal sequence helps in reducing the training time of our classifier, based on adaptive resonance theory neural networks. As a matter of fact, training time decreases by almost two orders of magnitude on a standard personal computer when the dimensionality of the classified set is increased from one to three images. This trend could have been forecasted by the corresponding increase of the HDI value: more discriminability means also that the neural classifier is faster in recognizing similarity and dissimilarity among inputs. We did not expect, however, that the decrease were roughly one order of magnitude for any new image added to the set.

Finally, we should note that, given the very basic class set we are dealing with, more than three images provide an HDI value equal to 100. This is visible in Fig. 5, where the trend for all the combinations of HDI is shown. Our explanation is that more than three images provide an input to the neural classifier which is redundant with respect to our classification task. However, such a "saturation effect" may mean that the sequence allows now discriminating more classes. As a matter of fact, using the whole sequence we found that it is possible to resolve partially the urban and suburban road map. So, in Fig. 4(c), we show the results obtained by classifying seven images and looking also for the street network. The definition of some features in the map

(a) (b) (c)

Fig. 4. Classification map for (a) the best single-date SAR image, (b) the best combination of two SAR images, and (c) the whole ERS-1/2 sequence [colors identify classes as in Fig. 1(b)].

TABLE II
CONFUSION MATRIX FOR THE JOINT CLASSIFICATION OF THE 1992 AND 1994 PREFLOOD ERS IMAGES, AND IMPROVEMENTS WITH RESPECT TO TABLE III

	Water	Veget.	Built area	*Omis. acc.*	*Improvements*
Water	5554	37	0	99.3%	+ 5.3%
Vegetation	2274	193028	3236	97.2%	+ 0.0%
Built area	71	11969	18467	60.5%	+ 5.2%
Comm. acc.	70.3%	94.1%	85.1%		
Improvements	+ 14.8%	+ 0.8%	-7.2%		

TABLE III
FUZZY ARTMAP CLASSIFICATION OF THE ERS-1 DATA ON AUGUST 13, 1992 (REPRINTED FROM [15])

	Water	Veget.	Built area	*Omis. acc.*
Water	5257	334	0	94.0%
Vegetation	4177	192958	1403	97.2%
Built area	37	13603	16867	55.3%
Comm. acc.	55.5%	93.3%	92.3%	

has dramatically improved with respect to single image classifications. In Fig. 4(c), the wide roads with trees following the ancient boundaries of the town can be more precisely individuated. In turn, this result improves characterization of the town structure, allowing a better definition of the boundaries between blocks, where roads are usually found.

The last note is that, while the accuracy improves, problematic areas are still present, even in the best classification map. For instance, the relative orientation among the streets and the sensor explains why some roads are not detected in Fig. 4(c). This effect would be partially solved by using both ascending and descending ERS images (currently all our scenes are descending), but only to a small extent. The possibility to provide images with different viewing angles, which is one of the possibility offered by ASAR and by the X-band sensors of the COSMO/SkyMed constellation, is more useful to this purpose.

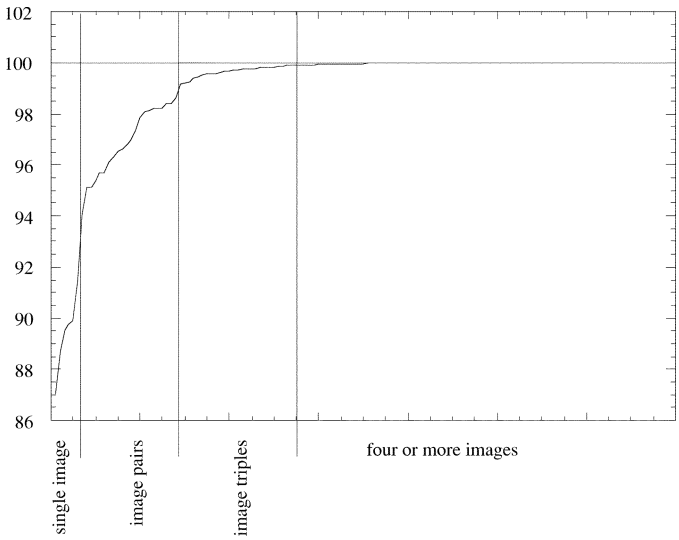

Fig. 5. (Left to right) HDI values for any combination of one, two, or more images of the ERS dataset over Pavia.

B. Road Map Extraction by Means of Multiangle SAR Images

Following the previous discussion, we show in Fig. 6(a) and (b), the two simulated COSMO/SkyMed SAR images, corresponding to orthogonal views of the center of Pavia and labeled as 0° and 90°. After a manual coregistration step, these images and the third one considered cover the same area and provide complementary information about the urban structure, as already discussed. This dataset is not suitable for direct multiband

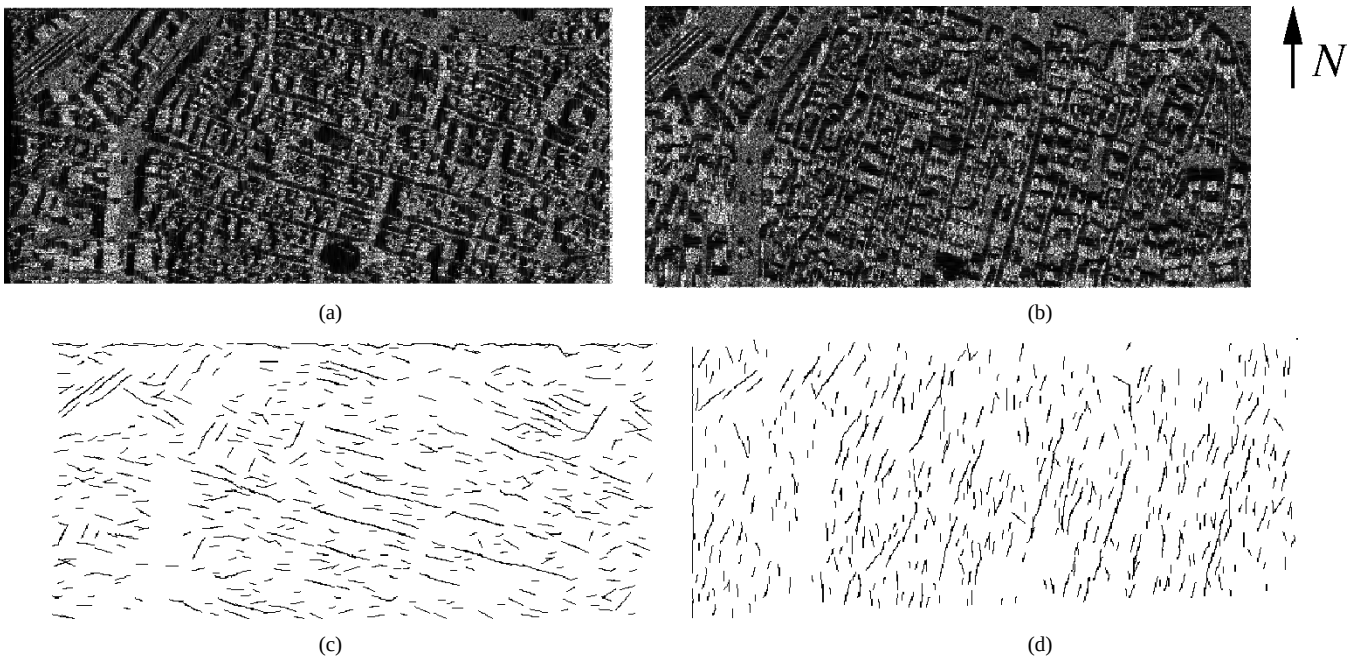

Fig. 6. (a) and (b) Simulated orthogonal X-band SAR views of central Pavia. (c) and (d) Street networks extracted from the same images by means of the FHT approach as in [16].

classification because the same buildings have different appearances in the two images, according to the sensor position. These images, instead, can be usefully integrated to characterize the road network inside the town, which is difficult to reconstruct entirely by means of a single SAR view even with a fine spatial resolution.

We, thus, applied to the simulated SAR images a road extraction procedure aimed at detecting straight and curvilinear objects in the scene, and investigated if we could use the results from these different views of the same area to overcome the cardinal effect, i.e., the different appearance of the street network due to the viewing geometry. Looking at the images, we observe that large outer boulevards always appear, while roads in the city center and finer details can be highlighted only by the joint use of more points of view. Moreover, this dataset can be useful to understand to what extent the problems in very dense urban areas already discussed in the previous paragraphs may be reduced using multiple views.

Road extraction on both images was performed using two fuzzy extractors proposed in [16]. The procedure requires a first classification step for a rough characterization of the scene in street/nonstreet pixels, followed by their clustering in consistent street segments. In [16], it was noted that it is difficult to have extraction routines well suited for any situation, and this is especially true in our test site, due to the complex structure of the town center. Among the proposed approaches, the fuzzy Hough transform (FHT) and the fuzzy shortest path extraction (FSPE) play here the most relevant roles, because of the complex shape of many roads. FSPE exploits *dynamic programming* [17] to find the path with the lowest cost going from one point to an other, where this cost is computed by means of the sum of the fuzzy membership values assigned to the path pixels by the previous classification step. To the aim of extracting more streets, in our implementation this path extraction is applied iteratively starting from each of the four sides of the image, and thresholds are set to take into account streets ending inside the area of interest. FSPE is a very flexible approach, but sometimes it fails, and reports false connections. Moreover, it suffers from occlusions and speckle noise in SAR images, that produces inconsistent pixel values and often leads to an interruption of the extracted path. It is however a very efficient way to extract clearly visible curvilinear roads. FHT instead is an adaptation of the well-known Hough transform to a fuzzy input. For example, FHT results at one threshold for Fig. 6(a) and (b) are shown in Fig. 6(c) and (d), respectively. Main roads with orthogonal orientation have been extracted by each image, and the two street networks highlight different parts of the same road map.

Our assumption is that if we apply a fusion process to the networks extracted from different images, we will improve the overall result. Therefore, we realized a feature fusion procedure. As a matter of fact, after obtaining the road network on a view by applying FHT or FSPE, with different thresholds and preprocessing steps, we may combine the results with many logical operators [18]. In this work, just to highlight the complementarity of the datasets at different views, we use a simple logical OR, followed by a pruning procedure to delete multiple detections of the same road. More in detail, the pruning procedure, which is an essential step in our algorithm, is based on the definition of a matrix where each row represents a segment or line and contains the number of the rows associated to the segments/lines "overlapping" with it. Specifically, two segments/lines are considered as overlapping if one of them has more than a given percentage (usually set to 70%) in the neighborhood of the other one, defined as the area obtained by thickening this segment/line by a given amount (according to spatial resolution, expected mean registration error, etc.). If two segments/lines are overlapping, only the longer one has its row updated in the matrix with the index of the other. This is made to preserve longer segments, that

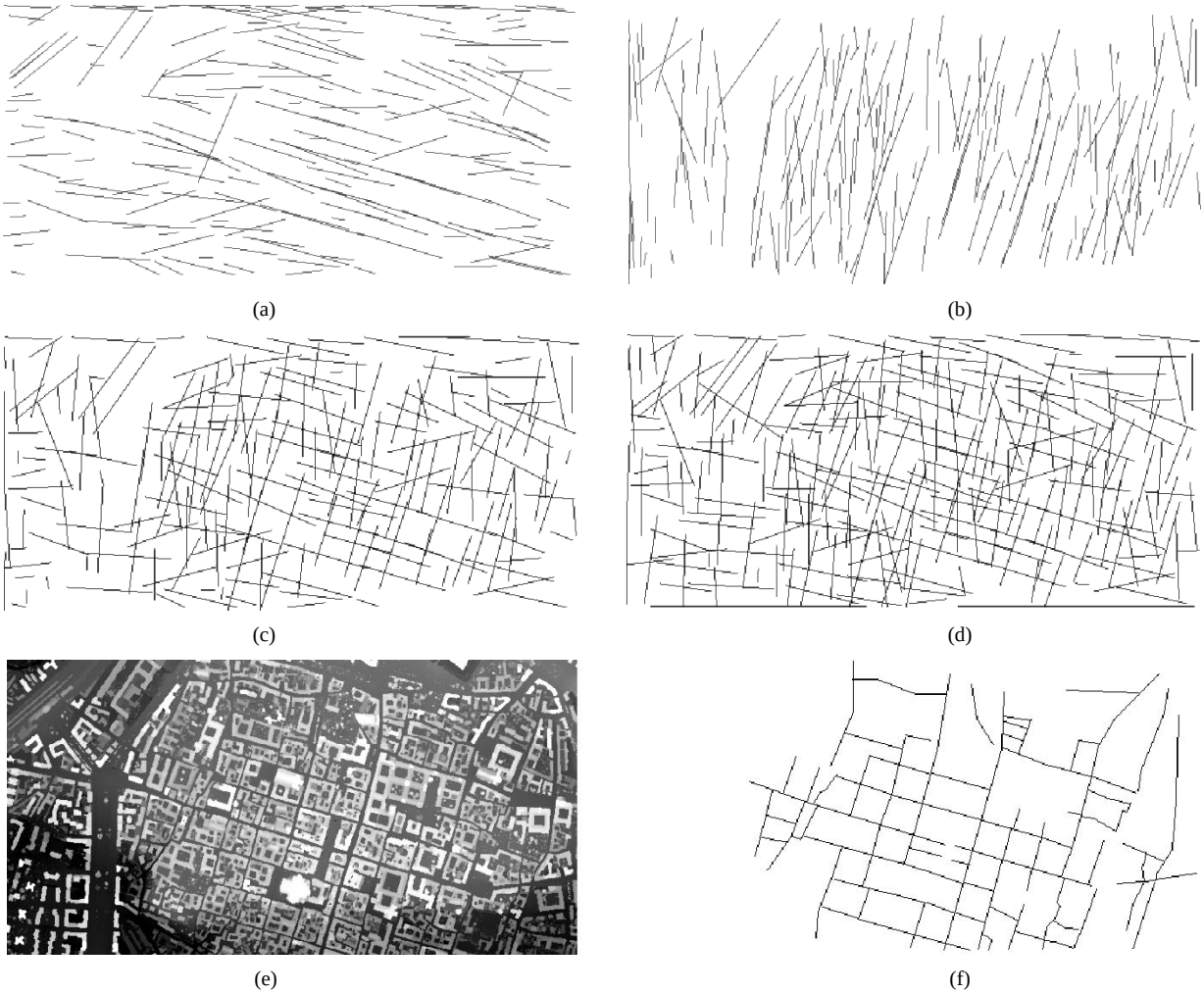

Fig. 7. (a) and (b) Street networks extracted by the proposed fusion process starting from the SAR images in Fig. 6(a) and (b). (c) Road map obtained by fusing street networks from two orthogonal views. (d) Road map obtained by fusing street networks from three SAR views. (e) Grayscale image of the LIDAR data over the same area. (f) Manually extracted road map of the city center.

corresponds to more important street portions. Finally, pruning is done by discarding those segments/lines that have no number in their row and whose index is in at least one other row in the matrix.

More refined road maps for Fig. 6(a) and (b) than those in Fig. 6(c) and (d) are shown in Fig. 7(a) and (b). Then, the same OR and pruning procedure was applied to these results to find a more complete network on the study area, which is shown in Fig. 7(c). Finally, we considered also the addition of the third image, and the combination of the three views is shown in Fig. 7(d). A first evaluation of the proposed procedure may be assessed by a comparison with available laser range (LIDAR) data in the same area [see Fig. 7(e)], clearly showing the actual road network. We observe that, starting from any of the two SAR images, the widest and longest roads orthogonal to the flight direction have been recognized. So, the combination of these two views allows extracting a rough but quite clear idea of the actual disposition of the streets in the city. Three views provide a better results, even if the advantage is not as relevant as in using orthogonal views. We should note, finally, that long roads are still fragmented, and false alarms, due to very complex scattering patterns in high-resolution SAR images, are present. So, in conclusion we may say that, although the merging process needs to be further improved using more refined fusion operators, results show that the use of more SAR views provides much better characterizations than considering one view at a time. The availability of more views improves (dramatically, in some parts of the image) the understanding of the scene.

The same observations stem from the numbers in Table IV, where we show quantitative evaluation indexes for single-view and multiview fusion of the street networks. These values were computed considering as ground truth a manually extracted road map, where only the streets in the city center have been considered, shown in Fig. 7(f). Note that this choice introduces somehow a bias in the values of these indexes, even if it allows a better comparison of the results. In Table IV, we introduce the indexes proposed in [19] to provide a more general characterization of a street network. They are *completeness*, the fraction of ground truth length extracted, *correctness*, the fraction of segments' length belonging to actual roads, *quality*, and *redundancy*. A first look to the values confirms that all these numbers validate our qualitative assessment. Completeness increases with the use of more SAR views, showing that more streets have been recognized, while correctness nearly remains

TABLE IV
EVALUATION INDEXES FOR STREET NETWORKS OBTAINED BY FUSION OF MULTIPLE SAR VIEWS OF THE SAME AREA

input view	correctness	completeness	quality	redundancy
0° data only	0.20	0.24	0.30	0.57
40° data only	0.23	0.28	0.31	0.74
90° data only	0.19	0.18	0.23	0.46
0° and 90° data	0.25	0.23	0.26	0.63
0° and 40° and 90° data	0.30	0.23	0.25	0.73

constant, because the false positive affect both images in the same way. Finally, redundancy increases, because different parts of the same road, found starting from different views, add up to a better recognition but also to a larger fragmentation of the achieved results.

IV. CONCLUSION

This work presents an investigation on the analysis of multiple SAR images recorded over the same urban site. We studied how the use of multitemporal and multiangle data may improve single-date/view urban characterization, and we have shown results using actual as well as simulated SAR images.

We found that a classification strategy based on HDI and a neural classification tool allows exploiting the temporal redundancy of a sequence of satellite SAR data. In turn, this stresses the fact that, using a sufficiently long temporal series of satellite measurements, an accurate characterization of stable features in urban environments is possible even with current earth science satellites. However, the coarse resolution is still a limit of these data, and future researches are needed to understand to which extent multitemporal redundancy may make for it.

Similarly, we have shown that more streets can be detected and extracted using multiple views of the same urban area by means of the same SAR sensor. This is a relatively new research field for urban remote sensing, although in other fields (like computer vision, for instance) the availability of such data has long be considered a useful source of information. For SAR data, the advantage of multiviewing analysis is usually related to the shadowing and layover effects that reduce the usefulness of single-view images.

One problem still to be addressed is the registration of the different SAR views. Current methods for coregistration are mainly based on cross correlation, but SAR data of the same area with different viewing angles are completely different. Moreover, building corners, that are usually chosen as ground control points, are reprojected in different positions in ground range images, because of the layover effect, depending also on the building height. So, an automatic system for coregistration is far from being operative, and in this research we operated manually. However, the point of semiautomatic coregistration of fine resolution SAR images deserves more attention, since these datasets are becoming more easily available. We are exploring the use of street crossing centers, which are at the ground level, so without any layover problem, or permanent scatterers as feature points to be coregistered.

ACKNOWLEDGMENT

The authors wish to thank D. Riccio and his group for providing the simulated X-band SAR data and G. Pulina for the programming work.

REFERENCES

[1] G. Nico, M. Pappalepore, G. Pasquariello, A. Refice, and S. Samarelli, "Comparison of SAR amplitude vs. coherence flood detection methods—a GIS application," *Int. J. Remote Sens.*, vol. 21, no. 8, pp. 1619–1631, 2000.

[2] F. Caltagirone, G. Manoni, P. Spera, and R. Vigliotti, "SkyMed/COSMO mission overview," in *Proc. IGARSS*, vol. 2, Seattle, WA, July 1998, pp. 683–685.

[3] R. W. Zahn and E. H. Velten, "Enabling technologies for the TerraSAR mission," in *Proc. IGARSS*, vol. 3, Honolulu, HI, July 2000, pp. 1174–1176.

[4] E. Costamagna, P. Gamba, V. Casella, A. Spalla, F. Casciati, S. Podestà, P. Ghilardi, and L. Natale, "A web based GIS archive for local area hazard prevention and mitigation," in *Proc. 6th GI/GIS Workshop*, Lyon, France, June 2000.

[5] G. Franceschetti, A. Iodice, D. Riccio, and G. Ruello, "An electromagnetic model for SAR raw signal simulation of urban areas," in *Proc. IEEE/ISPRS Joint Workshop on Remote Sensing and Data Fusion Over Urban Areas*, Rome, Italy, Nov. 8–9, 2001, pp. 10–14.

[6] S. Quegan, T. Le Toan, J. J. Yu, F. Ribbes, and N. Floury, "Multitemporal ERS SAR analysis applied to forest mapping," *IEEE Trans. Geosci. Remote Sens.*, vol. 38, pp. 741–753, Mar. 2000.

[7] P. Saich and M. Borgeaud, "Interpreting ERS SAR signatures of agricultural crops in Flevoland, 1993–1996," *IEEE Trans. Geosci. Remote Sens.*, vol. 38, pp. 651–657, Mar. 2000.

[8] H. Lee and J. G. Liu, "Analysis of topographic decorrelation in SAR interferometry using ratio coherence imagery," *IEEE Trans. Geosci. Remote Sens.*, vol. 39, pp. 223–232, Feb. 2001.

[9] S. Usai and R. Klees, "SAR interferometry on a very long time scale: A study of the interferometric characteristics of man-made features," *IEEE Trans. Geosci. Remote Sens.*, vol. 37, pp. 2118–2123, July 1999.

[10] S. Usai, "An analysis of the interferometric characteristics of anthropogenic features," *IEEE Trans. Geosci. Remote Sens.*, vol. 38, pp. 1491–1497, May 2000.

[11] A. Ferretti, C. Prati, and F. Rocca, "Permanent scatterers in SAR interferometry," *IEEE Trans. Geosci. Remote Sens.*, vol. 39, pp. 8–20, Jan. 2001.

[12] M. Pesaresi, "The remotely sensed city," JRC, Ispra, Italy, Post-Doctoral Fellowship Final Rep., Mar. 2000.

[13] P. Gamba and B. Houshmand, "An efficient neural classification chain of SAR and optical urban images," *Int. J. Remote Sens.*, vol. 22, no. 8, pp. 1525–1553, Aug. 2001.

[14] P. Gamba and F. Dell'Acqua, "Improved multiband urban classification using a neuro-fuzzy classifier," *Int. J. Remote Sens.*, vol. 24, no. 4, pp. 827–834, Feb. 2003.

[15] F. Dell'Acqua and P. Gamba, "Evaluation of COSMO/SkyMed SAR data for urban characterization," *Proc. IEEE/ISPRS Joint Workshop Remote Sensing and Data Fusion Over Urban Areas*, pp. 141–145, Nov. 8–9, 2001.

[16] ——, "Detection of urban structures in SAR images by robust fuzzy clustering algorithms: The example of street tracking," *IEEE Trans. Geosci. Remote Sens.*, vol. 39, pp. 2287–2297, Oct. 2001.

[17] M. Buckley and J. Yang, "Regularised shortest-path extraction," *Pattern Recognit. Lett.*, vol. 18, pp. 621–662, 1997.
[18] F. Dell'Acqua, P. Gamba, and G. Lisini, "Extraction and fusion of street networks from fine resolution SAR data," in *Proc. IGARSS*, vol. I, Toronto, ON, Canada, June 2002, pp. 89–91.
[19] C. Wiedemann and H. Ebner, "Automatic completion and evaluation of road networks," *Int. Arch. Photogramm. Remote Sens.*, pt. 3B, vol. 33, pp. 979–986, 2000.

Fabio Dell'Acqua (M'01) was born in Pavia, Italy, on March 28, 1971. He received the first-class honors and Ph.D. degrees in electronics engineering from the University of Pavia, Pavia, Italy. He passed the qualification exam for practicing the profession of engineer in November 1996.

He is currently working on processing and interpretation of satellite images. From 1996 to 1999, he attended a Ph.D. course in electronics and computer science engineering at the University of Pavia, investigating shape analysis techniques to process meteorological images. From September to December 1998, he was a Visiting Researcher at Colorado State University, Fort Collins, where he studied weather satellite imagery analysis. In the first half of 2000, he worked on analysis and reconstruction of range data (EU TMR—CAMERA) as a Research Associate at the Vision Laboratory, University of Edinburgh, Edinburgh, U.K. From July 2000 to November 2001, he was a Post Doctorate at the University of Pavia, where in December 2001, he received a permanent position as an Assistant Professor. His fields of interest include shape analysis, retrieval of images from archives, range data analysis, neural networks, and remote sensing.

Paolo Gamba (S'91–M'93–SM'00) received the laurea (cum laude) and the Ph.D. degrees in electronic engineering from the University of Pavia, Pavia, Italy, in 1989 and 1993, respectively.

He is currently Associate Professor of telecommunications at the University of Pavia. From 1992 to 1994, he was a Research and Development Engineer in the Microwave Laboratory of Siemens Telecomunicazioni, Cassina de' Pecchi, Milano, Italy. In 1994, he joined the Department of Electronics, University of Pavia, first as a Teaching Assistant and later as an Assistant Professor and now as an Associate Professor. Since 1997, he has been teaching radiocommunications systems, electrical communications, and remote sensing image processing. He has been involved in a number of projects funded by the European Community, the Italian Ministry for Scientific Research, the Italian Space Agency (ASI), and the Italian Research Council (CNR). From 1998 to 2001, he has acted as a Consultant for the Radar Science and Technology Section, Jet Propulsion Laboratory (JPL), Pasadena, CA, concerning SAR over urban areas. He is the Guest Editor of a special issue of the *ISPRS Journal of Photogrammetry and Remote Sensing* on "Algorithm and Techniques for Multi-Source Data Fusion in Urban Areas" and a special issue of the *International Journal of Information Fusion* on "Fusion of Urban Remotely Sensed Features." His current research interests include remote sensing data processing for urban applications, especially SAR urban analysis, multitemporal/polarization/frequency and multispectral data classification by neural and fuzzy classification tools, satellite image interpretation for civil protection purposes, weather radar, and meteorological satellite data interpretation.

Dr. Gamba was the recipient (first place) of the 1999 ESRI Award for Best Scientific Paper in Geographic Information Systems. He was also awarded a Fulbright grant for the academic year 1999/2000. He was the Organizer and Technical Chair of the first IEEE/ISPRS Joint Workshop on "Remote Sensing and Data Fusion over Urban Areas," whose first issue was held in Rome, Italy, in November 2001, and the second is in Berlin, Germany, in May 2003. He is a Guest Editor for this special issue of the IEEE TRANSACTIONS ON GEOSCIENCE AND REMOTE SENSING on "Urban Remote Sensing by Satellites." He is currently Chair of Technical Commette 7 "Pattern Recognition in Remote Sensing" of International Association for Pattern Recognition (IAPR) and is a member of the Data Fusion Committee of IEEE Geoscience and Remote Sensing Society.

Gianni Lisini was born in Voghera, Italy, on April 25, 1977. He received the laurea degree in electronic engineering from the University of Pavia, Pavia, Italy, in 2002. He is currently pursuing the Ph.D. degree in electronic engineering at University of Pavia.

His main interest involve image analysis, aerial and satellite data analysis over urban environments, and SAR remote sensing.